SIMULATION OF PSR INSTABILITY

Tai-Sen F. Wang

Los Alamos National Laboratory

Eighth Beam Dynamics Mini-Workshop on Two-Stream Instabilities in Particle Accelerators and Storage Rings

Hotel Loretto, Santa Fe, NM
February 16 - 18, 2000

Abstract

Evidences have been collected to support the theory that the instability in the PSR is an electron-proton (e-p) two-stream instability. This present work is a computer simulation study of the e-p instability in the PSR. The simulation is based on numerical solutions of the equations describing the motion of proton beam's centrod and the motion of macro-particles representing the trapped electrons. The study takes into account the effects of variable line densities as well as the secondary emission and the multipacting of electrons. The simulation results agree well qualitatively with experimental observations and earlier simulations using the centroid model. It is found that with only a few percent neutralization, the PSR beam can become unstable. It is also found that the enhancement of the instability due to the electron multiplication may occur after the oscillation of the proton beam has grown to large amplitude.

1 Introduction

Evidences have been collected to show that the PSR instability is an *e*-*p* instability.

The same kind of instability has been previously observed in Bevatron and ISR.

The basic mechanism of the instability has been understood, the recent PSR upgrade as well as SNS and ESS are calling for more detailed understandings.

Earlier simulation program using the centroid model has recently been modified:

- replace the electron centroid by macro-electrons,
- include the secondary emission of electrons due to the impact of electrons on the beam pipe.

The present emphasis is to study the possibility of multipacting and the effect of electron multiplication on the instability.

2 The Model and the Numerical Approach

2.1 Model

A proton bunch of length L with a round cross-section of radius a, traveling with a constant speed v inside a perfect conducting pipe of radius b.

Linear transverse focusing on protons. Uniformly distribution of protons in the transverse direction.

The proton bunch is partially neutralized by electrons.

Use a Cartesian coordinate system:

z axis parallel to the proton beam,
y axis perpendicular to the ring,
origin at the center of the beam cross section.

Proton and electron line-densities, λ_p and λ_e, depend on z.

Assume the system is unstable in the y-direction only.

Neglect the axial motion of electrons and the synchrotron oscillation of protons.

Study the motion of the proton beam centroid $Y_p(z,t)$ = averaged displacement of protons at (z,t), where t = time.

Equation of motion for $Y_p(z,t)$:

$$\left(\frac{\partial}{\partial t} + v\frac{\partial}{\partial z}\right)^2 Y_p + \omega_\beta^2 Y_p = \frac{1}{\gamma}\sum_{j=1}^{n_e}\frac{F_{ej}}{m_p} - C_d\left(\frac{\partial Y_P}{\partial t} + v\frac{\partial Y_P}{\partial z}\right) \quad , \tag{1}$$

ω_β = betatron frequency due to the external focusing,
F_{ej} = force due to the jth electron,
$\gamma = (1 - v^2/c^2)^{-1/2}$,
c = speed of light,
m_p = rest mass of a proton,
C_d = damping constant .
The 2nd term on the RHS is due to the damping caused by the tune spread.

Neglect the interaction among electrons.

Equation of transverse motion for the jth electron at (y_{ej}, z):

$$\frac{d^2 y_{ej}}{dt^2} = \frac{F_p(y_{ej}, z, t)}{m_{ej}} \quad , \tag{2}$$

$F_p(y_{ej}, z, t)$ = the force due to the proton beam,
m_{ej} = the mass of the jth electron.

2.2 Numerical Approach

Computations are carried out on the moving frame of protons.

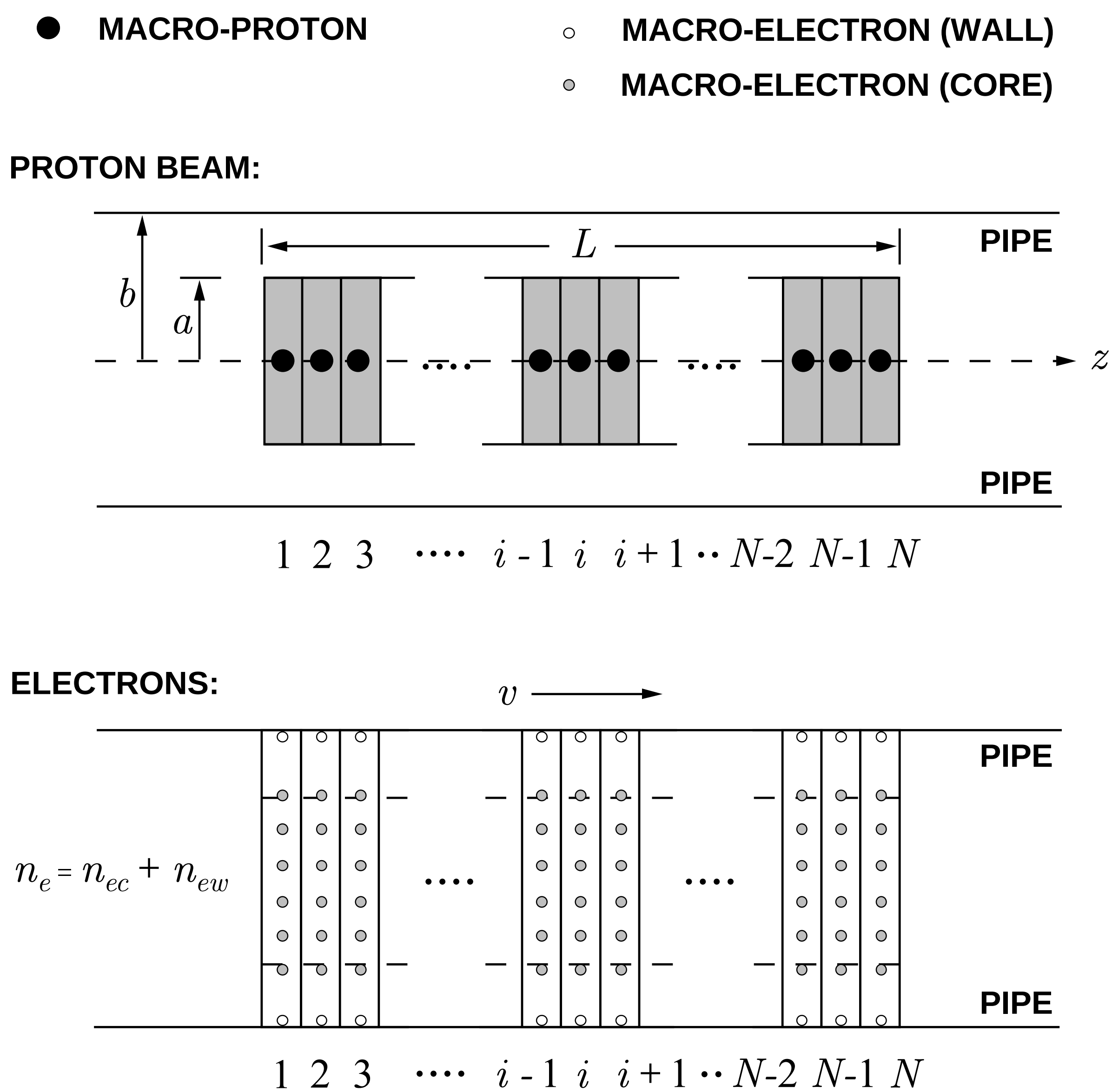

Fig. 1: Schematic of the computation setups.

The proton bunch and the electron cloud are divided into N slices (grids) each in the z-direction.

Each proton slice contains one macro-proton. The charges and the masses of macro-protons are assigned according to $\lambda_p(z)$.

Each electron slice contains n_e macro-electrons.

At creation, electrons have two components:
the wall-electrons (from wall) n_{ew}, charge c_w, mass m_{ew},
the core-electrons n_{ec}, charge c_c, mass m_{ec},
$n_e = n_{ec} + n_{ew}$.

The acceleration of the jth macro-electron due to the field of protons is approximated by

$$\frac{F_p(y_{ej}, z)}{m_{ej}} \approx \begin{cases} \dfrac{-e^2 q_j \lambda_p}{2\pi\epsilon_o m_{ej}} \left(\dfrac{Y_p}{b^2 - y_{ej} Y_p} + \dfrac{y_{ej} - Y_p}{a^2} \right), & \text{for } |y_{ej} - Y_p| \leq a, \\ \dfrac{-e^2 q_j \lambda_p}{2\pi\epsilon_o m_{ej}} \left(\dfrac{Y_p}{b^2 - y_{ej} Y_p} + \dfrac{1}{y_{ej} - Y_p} \right), & \text{for } |y_{ej} - Y_p| \geq a, \end{cases} \tag{3}$$

$e =$ unit charge,
$q_j =$ (total charge of the jth macro-electron)$/e$, a variable,
$\epsilon_o =$ permittivity of the free space,
$eq_j/m_{ej} = e/m_e =$ const..

The force on a macro-proton due to the jth macro-electron is approximated by

$$F_{ej} \approx \begin{cases} -\dfrac{e^2 q_j \lambda_p}{2\pi\epsilon_o}\left(\dfrac{y_{ej}}{b^2 - y_{ej}Y_p} + \dfrac{Y_p - y_{ej}}{R_e^2}\right), & \text{for } |Y_p - y_{ej}| \le R_e, \\ -\dfrac{e^2 q_j \lambda_p}{2\pi\epsilon_o}\left(\dfrac{y_{ej}}{b^2 - y_{ej}Y_p} + \dfrac{1}{Y_p - y_{ej}}\right), & \text{for } |Y_p - y_{ej}| \ge R_e, \end{cases} \tag{4}$$

R_e = "macro-electron radius" used to avoid singularity.

Eqs. (1) and (2) are solved by using Runge-Kutta-Gill method.

Time step: $\Delta t = L/(vN)$.

To simulate the relative drift of electrons:

In every Δt, advance all electron slices by one grid toward the tail of the proton bunch and create a new slice at the head of the proton bunch.

To simulate the electron generation due to the lost protons:

At every time step, use random number to select a slice in which two wall-electrons are created on the beam pipe.

Total number of macro-particles = const. all the time.

To model the accumulation of electrons from gas scattering:

Introduce a weight function $W_e(z)$ for the charge and the mass of macro-electrons according to

$$q_j = q_j(z,t) = c_j(z,t)W_e(z) \quad . \tag{5}$$

For constant electron generation per proton, then roughly,

$$W_e(z) \propto k + \int_0^z \lambda_p(z')dz' \quad . \tag{6}$$

To simulate the secondary emission on the wall:

When an impact is detected, q_j and m_{ej} of the impinging macro-electron is adjusted (q_j/m_{ej} = const.) according to the secondary emission yield (SEY).

Assuming normal incident, the SEY is calculated using:

$$\delta_{ts}(E_0/\theta_0) = \hat{\delta}(\theta_0)D(E_0/\hat{E}(\theta_0)) \quad , \tag{7}$$

where

$$D(x) = \frac{sx}{s-1+x^s} \quad , \tag{8}$$

$\delta_{ts}(E_0/\theta_0)$ = SEY,
E_0 and θ_0 = energy and incident angle of the electron,
$\hat{E}$ = energy at maximum D, $s \approx 1.44$,
$\hat{\delta}$ = maximal SEY at θ_0.

3 Examples of Numerical Results

3.1 Example A: PSR with a clean gap

Assume a parabolic proton line-density,

$$\lambda_p(z) = 6N_p s(1-s)/L \quad , \tag{9}$$

and a weight function

$$W_e(z) = 0.1 + 1.8s^2(3-2s)\,, \quad \text{so that } W_e(L/2) = 1\,, \tag{10}$$

$s = z/L$, $z =$ axial distance from the head of the bunch.

$L/v \approx 260$ns for PSR.

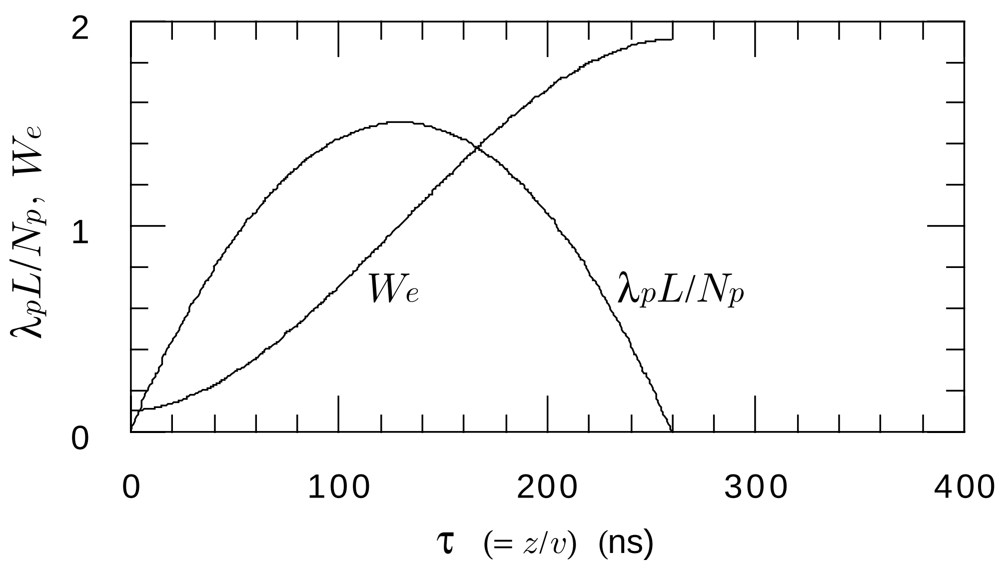

Fig. 2: The proton line density λ_p (normalized by N_p/L) and the electron weight function W_e considered in the examples. The gap is between τ = 260 ns and τ = 360 ns.

Initial fraction of neutralization, $\chi \approx 4\%$ at $z \approx 0.5L$.

PSR parameter values: $\gamma = 1.85$, $a = 1.5$cm, $b = 5$cm, circumference $C = 90$m, $N_p = 2.6 \times 10^{13}$, and $\nu_y = 2.3$.

The maximal electron bouncing frequency at these parameter values ≈ 185 MHz.

Chose $N = 520$, $\Delta t = 0.5$ns, and $C_d = 5 \times 10^4$/s.

Assume initially $Y_p(z, 0) = 0.076 \sin[(\pi z)/\text{m})]$cm, and $dY_p/dt = 0$.

Corresponds to a wave of 126 MHz when carried by the traveling proton beam.

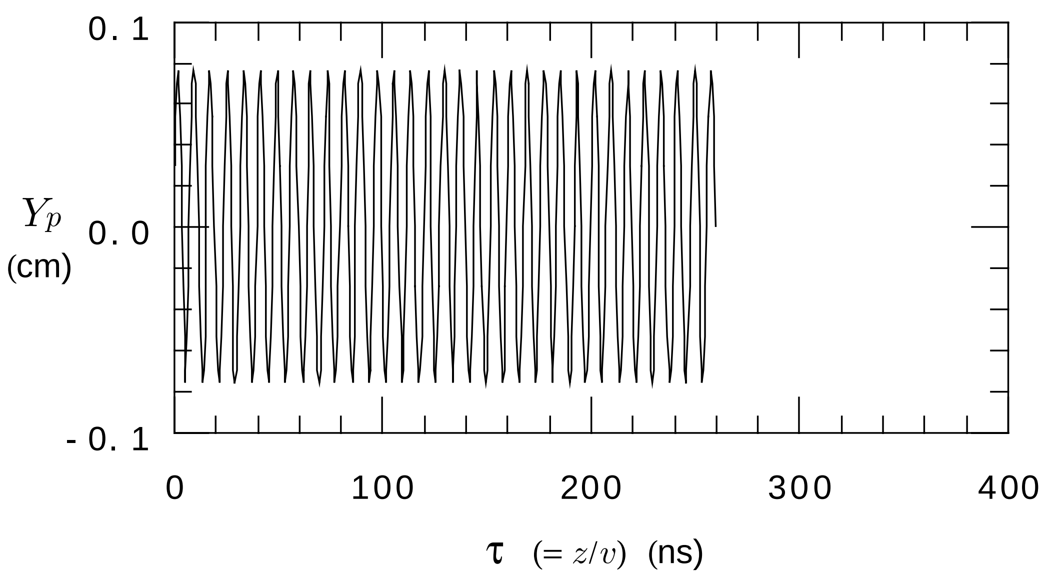

Fig. 3: The initial perturbation on Y_p .

Initially, 23 core-electrons and 2 wall-electrons per slice, evenly distributed from wall to wall (-5cm to 5cm).

Maximum number of macro-electrons per slice = 29.

All electrons start at rest, and $R_e = 0.7$cm.

Initial charge assignment of macro-electrons:

$$c_c = [e\lambda_p\chi/(n_{ec} + 0.5n_{ew})]_{z=L/2}\ , \quad \text{and} \quad c_w = c_c/2\ .$$

For wall-electrons created by protons after $t = 0$:

$$c_w = c_c(t = 0)/2\ .$$

Secondary Emission: $\hat{\delta} = 2.0$, $\hat{E} = 295$eV.

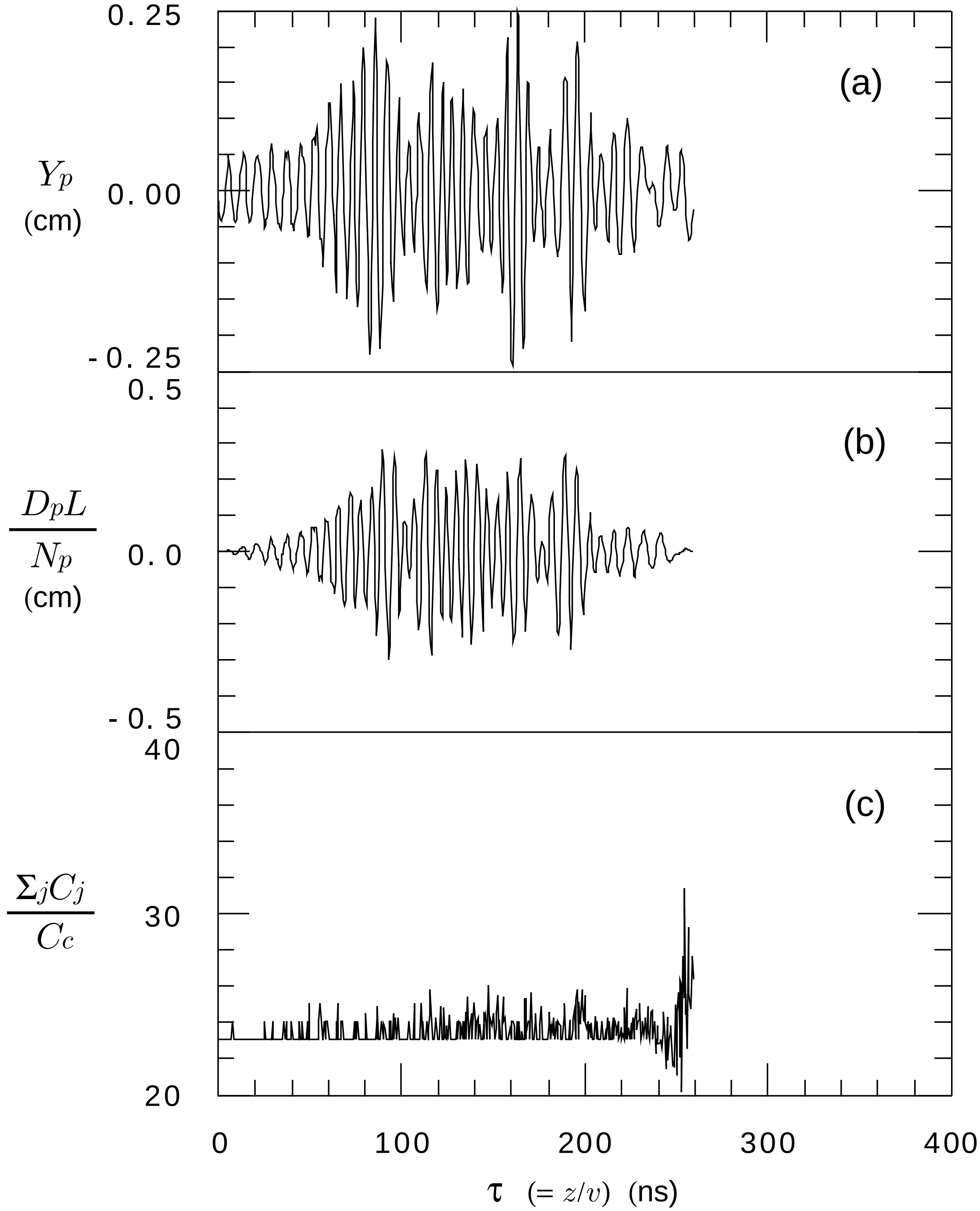

Fig. 4: (a) A snapshot of Y_p taken after tracking motion for 30 proton revolutions in the PSR ($\approx 10.8\mu$s), (b) the dipole moment density $D_p = \lambda_p Y_p$ at the 30th revolution shown after normalization by N_p/L, and (c) the snapshot of the quantity $\sum_j c_j/c_c$ along the proton bunch taken at the same time as Y_p $\left(\sum_j c_j/c_c > 26 \Rightarrow \text{electron multiplications}\right)$.

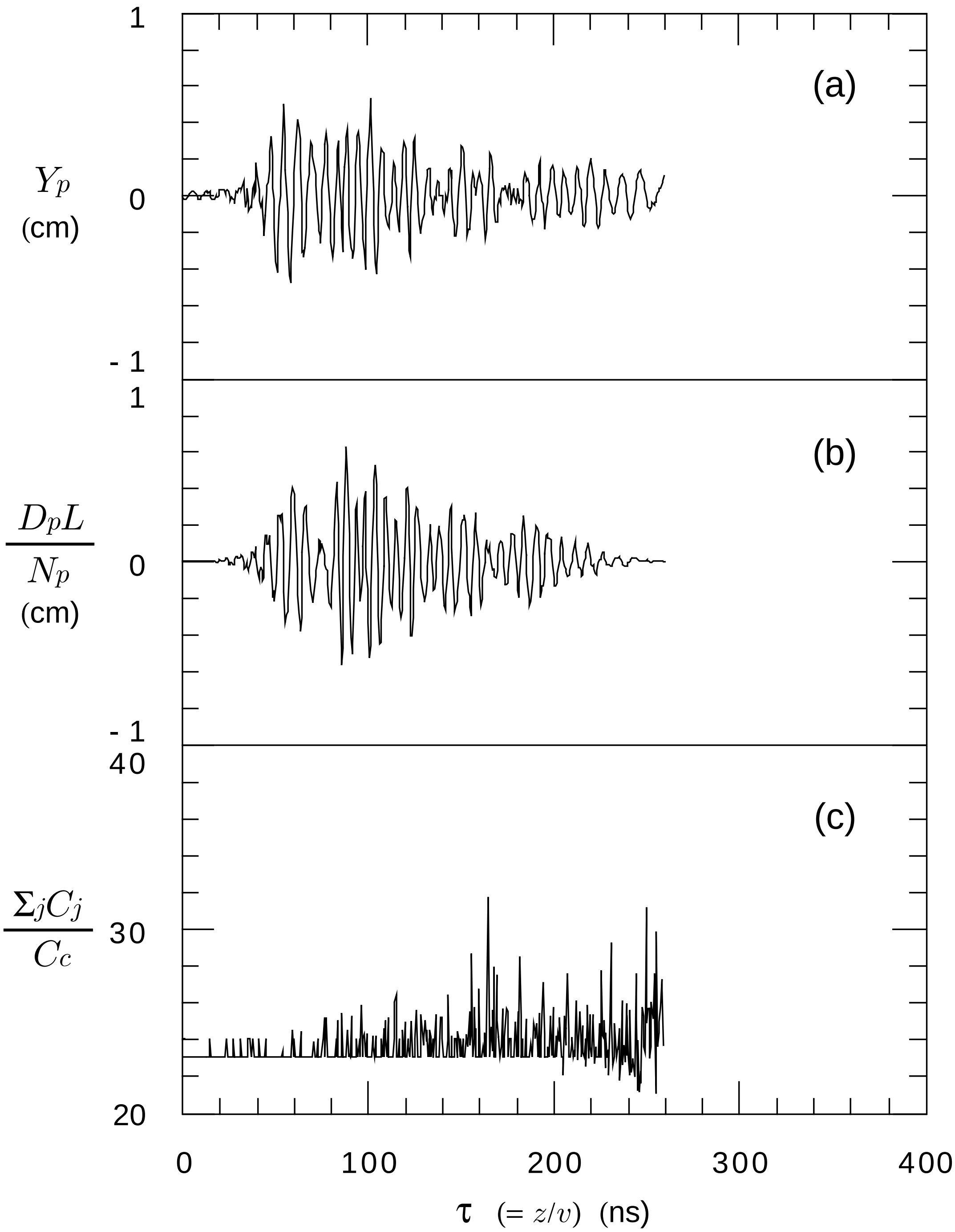

Fig. 5: (a) A snapshot of Y_p taken after tracking motion for 120 proton revolutions in the PSR ($\approx 43.2\mu$s), (b) the dipole moment density $D_p = \lambda_p Y_p$ at the 120th revolution shown after normalization by N_p/L, and (c) the snapshot of the quantity $\sum_j c_j/c_c$ along the proton bunch taken at the same time as Y_p $\left(\sum_j c_j/c_c > 26 \Rightarrow \text{electron multiplications}\right)$.

3.2 Example B: Multiplication threshold

Use the same initial conditions as in Example A but smaller perturbation.

Vary the beam intensity and check every time step in first turn to look for possible electron multiplication.

Observed multiplication at the tail of the bunch when $N_p \geq 1.3 \times 10^{13}$.

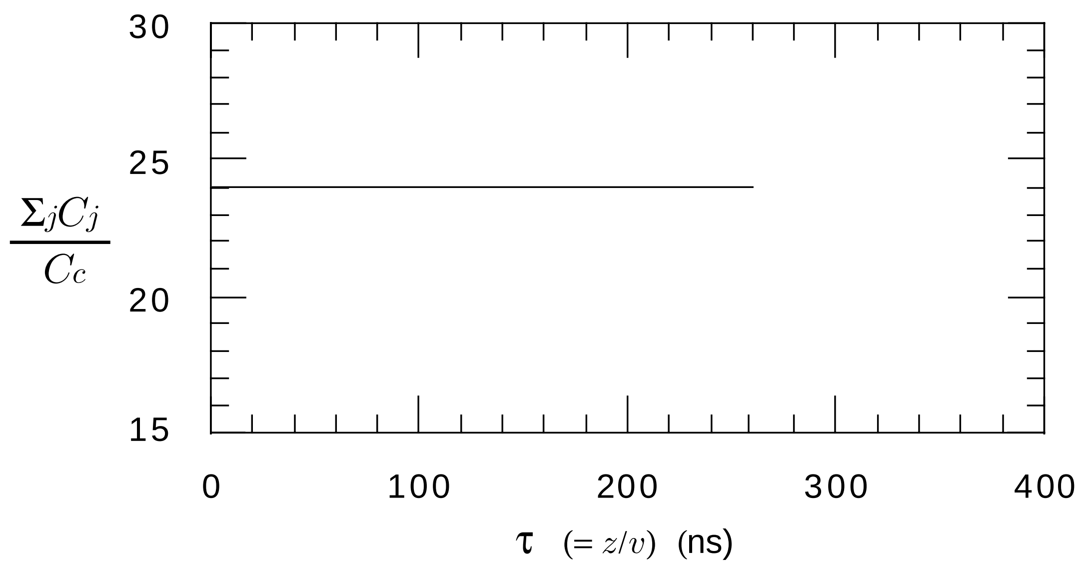

Fig. 6: The initial condition of the quantity $\sum_j c_j/c_c$ (proportional to the real number of electrons) as function of the time behind the head of the proton bunch. The system parameter values are the same as in the last example.

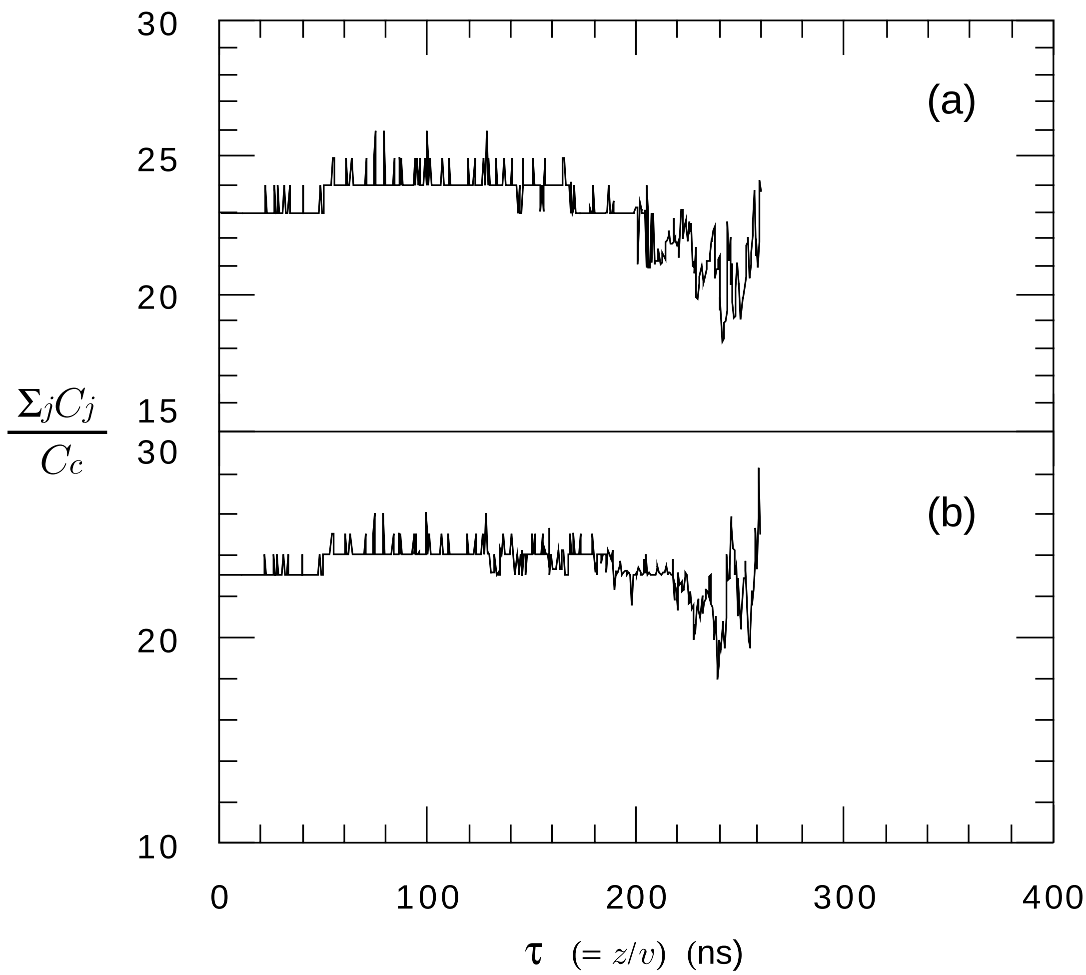

Fig. 7: The quantity $\sum_j c_j/c_c$ as function of the time behind the head of the proton bunch for (a) below and (b) above the multipacting threshold. The system parameter values are the same as in the last example. $N_p \approx 1.04 \times 10^{13}$ in (a) and $N_p \approx 1.69 \times 10^{13}$ in (b). The threshold is about $N_p \approx 1.3 \times 10^{13}$. Above the threshold, electron multiplications ($\sum_j c_j/c_c > 26$) occur in the tail of the proton bunch.

3.3 General Results

- It takes only a few percent neutralization for *e*-*p* instability to develop in PSR.

- Computed short growth time consistent with observations.

- An empty gap does not always ensure stability. Multi-turn trapping of electrons is not a necessary condition for instability.

- Roughly, the wavelength (or frequency) of the *e*-*p* oscillation $\propto \sqrt{\lambda_p}$. Wide frequency spectrum for non-uniform λ_p.

- The instability grows in time and in space.

- For stainless steel SEY of $\hat{\delta} = 2.0$ at $\hat{E} = 295$eV, multipacting initially occurs only in the tail of the proton bunch.

- Appreciable multipacting occurs in the middle and the later part of the bunch after proton oscillation has grown to large amplitude (> 0.5cm).

4 Conclusions

- Numerical simulations have been carried out for the *e*-*p* instability of the PSR beam by solving the equations of motion for the centroid of the proton beam and macro-electrons.

- Updated simulations include the production of secondary electrons on the beam pipe.

- Results are consistent with the earlier simulations using the centroid model and are qualitatively in good agreement with experimental observations.

- A few percent of neutralization is sufficient for the *e*-*p* instability to develop in PSR. Computed short growth time consistent with observations.

- An empty gap does not always ensure stability. Multi-turn trapping of electrons is not a necessary condition for instability.

- For stainless steel SEY of $\hat{\delta} = 2.0$ at $\hat{E} = 295$eV, multipacting initially occurs only in the tail of the proton bunch. For PSR, the threshold for multiplication is about $N_p \geq 1.3 \times 10^{13}$. Appreciable multipacting occurs in the middle and the later part of the bunch after proton oscillation has grown to large amplitude (> 0.5cm).